Optimization of low carbon fuels operation on a CI engine under a simplified driving cycle for transportation de-fossilization

Fuel
Volume 310, Part A, 15 February 2022, 122338
https://doi.org/10.1016/j.fuel.2021.122338

Antonio García*, Javier Monsalve-Serrano, David Villalta and María Guzmán-Mendoza

CMT - Motores Térmicos, Universitat Politècnica de València, Camino de Vera s/n, 46022 Valencia, Spain

Corresponding author (*):

Dr. Antonio García (angarma8@mot.upv.es)

Phone: +34 963876574

Fax: +34 963876574

Abstract

The study of internal combustion engines, and their associated energy conversion processes, is currently focused on targeting the reduction of pollutant emissions while maintaining or improving efficiency and fuel consumption. The research of alternative fuels, in particular low carbon fuels (LCF), seems to be a promising strategy for solving this problem. However, the characterization of a fuel with properties different than those of diesel requires numerous tests and resources to prove the viability of the substitution for another alternative. In Europe, for a vehicle to be homologated the World harmonized Light vehicles Test Cycle (WLTC) must be complied with. This cycle requires transient tests, that performed with a fuel for which an engine calibration is not yet existent would be difficult and could hinder the evaluation of the potential of a given fuel. This study proposes a cycle simplification methodology that seeks to reduce the driving cycle to a discrete set of stationary conditions, for which each operational calibration can be optimized. The optimization methodology is based on statistical analysis and modelling, and is presented to select the most desirable operating condition that can be reached using an LCF. For each testing point optimization NOx, soot, brake efficiency and fuel consumption are used as targets. Finally, the calibrated operating conditions are applied within the simplified cycle to assess the homologation potential of the studied fuel, as well as the equivalent CO_2 emissions under the criteria of a well-to-wheel analysis (WTW).

Keywords

Low carbon fuel; engine optimization; WLTC; well-to-wheel; homologation; statistical model

1 Introduction

Modern society is reliant on vehicles for the transportation of their individuals and their goods. However, the road transport sector is one of the main sources of greenhouse gas emissions [1]. Passenger vehicles in particular account for a significative percentage of the total automotive fleet, and thus their polluting effect is aggravated by their quantity. Recent years have shown the start of a transition towards the electrification of vehicles, which is considered as a pathway for the de-fossilization of the whole sector, through the use of electricity from low-carbon sources. The prospect is promising due to the rapid growth of renewable energy capacity [2], the cost reduction of greener technology against more contaminant energy production methods [3], and the general acceptance of the consumer to the use of electricity sources like wind and solar [4]. Under this panorama, and with policies supporting and accelerating the adoption of electric vehicles (EV) [5], the intention is to phase-out internal combustion engines (ICE) in vehicles by as early as 2030 [6]. Nonetheless, complete adoption of EVs will probably take longer because complete vehicle fleet replacements are estimated to occur every twenty years, and calculations indicate that even if half of new car sales were electric by 2035 only 30% of vehicles would be EVs [7]; some projections even indicate the proportion of EVs in the road vehicle fleet will be much lower (7% by 2030 [5]). Knowing that ICEs will still account for a significative percentage of all vehicles in the near-to-medium term future, it is important to evaluate alternatives for road transport energy carriers that can help reduce the pollution caused by combustion vehicles while they are still in use. Of those alternatives, low-carbon fuels (LCF) represent an interesting option because they provide the additional potential of being implemented under existent commercially available powertrain systems, while at the same time reducing the carbon dioxide lifecycle footprint of the fuel.

Alternative fuels for ICEs have been of interest for researchers since the first iterations of the engine. In recent years the focus on fuels not coming from fossil sources has increased due to the need of the sector to reduce CO_2 emissions and mitigate other pollutant emissions -such as NOx, CO, unburned hydrocarbons (HC) and particulate matter (PM)- that can harm both the environment and human beings. Additionally, these pollutants specifically regulated under norms such as Euro 6 [8]. LCF are a good alternative because they can be synthetized from carbon, separated from captured atmospheric CO_2 [9], and hydrogen from water electrolysis [10] (which can be obtained from processes that use surplus electricity from renewable sources); or come from biomass sources [11], as is the case for biofuels. For this study a LCF blend with biofuel content, composed of hydrogenated vegetable oil (HVO) and fatty acid methyl esters (FAME) is going to be used. The biofuel, in addition to the contribution with the reduction of the equivalent CO_2 released can have properties that aid in the reduction of NOx, HC and CO emissions, such as a lack of sulfurs and aromatics [12].

Different kinds of studies have been performed to evaluate ICEs. Some studies like the one on [13] tested LCF blends with OMEx and HVO to characterize the combustion, performance, and emissions by varying the composition of the blend at different speed and loads. Other studies on biofuels and CI engines in general focus on the effect of the variation of a single parameter on the combustion and emissions of the engine, like the work of [14] [15] [16]. Due to the complexity of the combustion process, works where several parameters are studied simultaneously require the approximation of models to explain the effects of the variations observed. The models are empirical simplifications of the phenomenon at hand and have already been proven effective in the study of internal combustion vehicles. The work of [17], for example, studied the effect of a gasoline-methanol mixture combined with metal nanoparticles by employing statistical analysis to see the effect the throttle position, the engine speed and the presence of nanoparticles had on the performance and emissions of spark-ignition (SI) engine. Statistical models have also already been employed for Diesel engines calibration in the work of [18] finding that this kind of models can accurately predict different responses of the engine with generalizable results. The final kind of study to evaluate internal combustion vehicles comprehends the adherence to regulations and the effect on driving conditions. For these studies, tools like GT-Power have often been employed as they can simulate driving conditions from stationary engine measurements as well as test hybrid and fully electric powertrains to have a complete comparison [19]. Other methodologies to assess probable driving scenarios can be seen in the form of the discretization of a complete driving cycle into discrete operating conditions [20], as is performed in this work.

After an overview of the current automotive scenarios where ICEs will continue to have an important role, the potential of LCF to reduce both equivalent CO_2 emissions and criteria pollutants, and the different studies methodologies capable of evaluating and characterizing ICEs it is worth continuing the developing of works to further the investigation on the improvement of ICEs. This work evaluates the use of an LCF with moderate renewable content, inside a light-duty compression ignition (CI) engine and proposes a simplified methodology for its assessment and operation calibration within a statistical model framework that can be replicated for the study of other fuels with different renewable content proportions and intensive properties. The application of a simplified driving cycle assessment allows for the detailed study of the parameter modifications in ICEs because only a reduced set of experiments is needed to estimate the cycle results. Thus, for each of the operating conditions, complete optimization procedures based on statistical analysis can be done, obtaining relevant information on the combustion and operation parameters while allocating time and resources efficiently.

2 Materials and methodology

2.1 Engine characteristics and test cell description

Table 1 Engine characteristics

General characteristics	
Number of cylinders [-]	4
Cylinder diameter [mm]	79.7
Stroke [mm]	80.1
Total displaced volume [cm^3]	1598
Connecting rod length [mm]	140
Compression ratio [-]	16.0
Rated power [kW]	100 @ 4000 rpm
Rated torque [Nm]	320 @ 2000 rpm

Injection system characteristics	
Type of injector	solenoid
Number of holes [-]	7
Hole diameter [µm]	141
Flow number [FN]	340
Maximum injection pressure [bar]	2000

A 4-cylinder commercially available 1.6 L CI engine provided with high-pressure EGR was used to perform this investigation. More information on the engine can be found in Table 1, including the type of injectors and compression ratio. The ECU was originally provided with a baseline diesel B7 calibration, which through an INCA V5.2 virtual environment (dedicated tool for ECU tests, diagnostics and calibration of electronically controlled systems in the vehicle [21]) was modified in 8 main parameters to achieve the desired calibration for the air management and injection systems. The parameters to be controlled during tests were the fuel mass injected, the injection pressure, the start of injection (SOI), the pilot injections fuel mass and dwell times, the in-cylinder cycle air mass and boosting pressure.

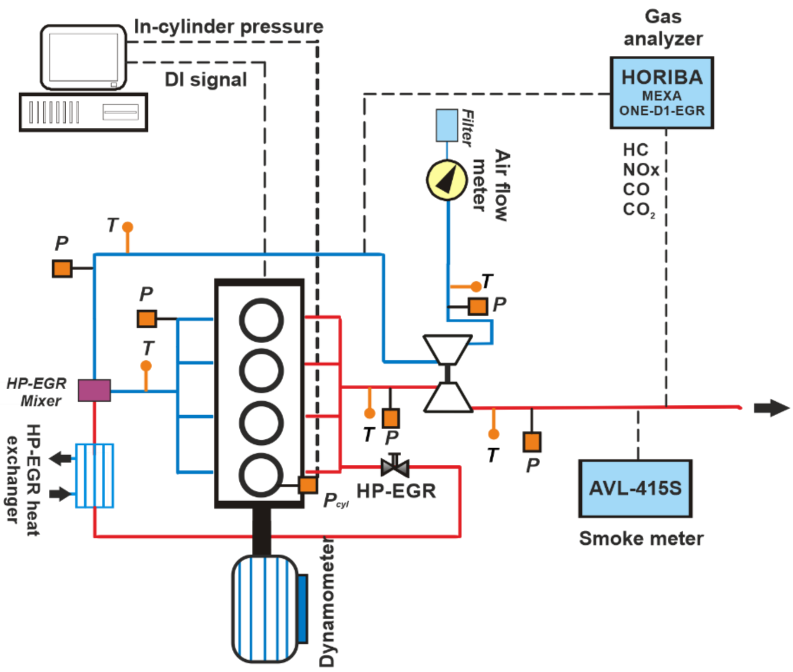

Figure 1 Test cell scheme

The engine was installed in a completely instrumented test rig, provided with a Dynas$_3$ LI dynamometer to measure the torque output, an Horiba MEXA 7100 to collect information on the main engine-out emissions of interest (NOx, CO, HC, O2 and CO_2), an AVL 415S smoke meter to measure soot in FSN number, and an air flow meter and a fuel balance to measure fuel mass flow. Additionally, pressure and temperature probes were present at the positions identified in Figure 1. The temperature and pressure values were recorded by an in-house LABVIEW controller, called CMT samaruc, which averaged the measurements. More information on the measuring equipment can be found in Table 2, including the accuracy each instrument has.

Table 2 Instrumentation accuracy

Variable measured	Device	Manufacturer/ model	Accuracy

In-cylinder pressure	Piezoelectric transducer	Kistler / 6125C	± 1.25 bar
Intake/Exhaust pressure	Piezoresistive transducers	Kistler / 4045A	± 25 mbar
Temperature	Thermocouple	TC direct / type K	± 2.5 ºC
Crank angle, engine speed	Encoder	AVL / 364	± 0.02 CAD
NOx, CO, HC, O2 and CO_2	Gas analyzer	Horiba MEXA 7100	4%
FSN	Smoke meter	AVL 415S	±0.025 FSN
Fuel mass flow	Fuel balance	AVL 733S	±0.2%
Air mass flow	Air flow meter	AVL 422	±0.1%
Torque	Dynamometer	$Dynas_3$ LI	

2.2 Fuel characteristics

This study is divided in two sections which will be performed with two fuels with different proportions of EU fossil diesel and renewable content. The first fuel is EU fossil diesel, while the second blend has 33% renewable content, with a composition of 7% FAME and 26% HVO. Some important properties of the studied fuel blends are present in Table 3. The fuel blends have different cetane index where the LCF blend has a higher value which will reduce the combustion delay time. As can be seen, the fuels have a similar energy density due to their similar carbon, oxygen and hydrogen content; however, as they are not identical in terms of lower heating value (LHV), equation 1 is used to obtain the equivalent fuel consumption excluding the effect of the lower heating value and using diesel as the reference and assessing the energy conversion each fuel blend can have; where $\dot{m}$ is the mass flow rate of fuel, and P_{brake} is the brake power.

$$BSFC_{eq}\left[\frac{g}{kWh}\right]=\frac{\dot{m}\cdot\left(\frac{LHV_{fuel\ blend}}{LHV_{Diesel}}\right)}{P_{brake}} \quad (1)$$

Table 3 Fuel properties at standard conditions

	Diesel blend	LCF blend
EU fossil diesel composition [%v/v]	93	67
FAME [%v/v]	7	7
HVO [%v/v]	0	26
Cetane Index [-]	54.6	62.4
Density @ 15ºC [g/ml]	0.834	0.821
KV @ 40ºC [cSt]	2.86	2.90
Water content [ppm = 100 %m/m]	80.0	0.012
Lower Heating Value [MJ/kg]	42.81	43.04
Carbon [% m/m]	85.78	85.40
Hydrogen [% m/m]	13.45	13.84
Oxygen [% m/m]	0.77	0.76
Residue [%vol.]	1.30	1.4
K_{CO_2} [g_{CO2}/g_{fuel}]	3.22	3.13
TTW CI [g_{CO2}/MJ]	75.2	72.7

WTT CI [g_{CO2}/MJ]	15.8	-6.7

The fuels' Well-to-Tank (WTT) carbon intensity was derived from the work performed in [22], while the Tank-to-Wheel (TTW) CO_2 emissions come from equations 2 and 3, under the premise of complete combustion. On equation 2, k_{CO_2} is the coefficient of correlation of a unit of mass of fuel into a unit of mass of CO_2, $y_{C_{fuel\,blend}}$ is the carbon proportion of the fuel in mass, while M_C and M_{O_2} are the molar masses of carbon and oxygen respectively. Then, on equation 3, $\dot{m}_{CO_2}$ represents the CO_2 mass flow rate. These equations provide a relation between the available carbon content in the composition of the fuel and the tailpipe CO_2. The hypothesis is supported, in part, by the high efficiency (above 90% [23] [24]) that can be obtained in diesel oxidation catalysts (DOC) which would make possible the complete oxidation of the fuel after the engine; additionally, this consideration implies the worst case scenario for CO_2 emissions where all the fuel used in the engine is exhausted from the vehicle as CO_2.

$$k_{CO_2} = y_{C_{fuel\,blend}} \cdot \left(\frac{M_C + M_{O_2}}{M_C}\right) \tag{2}$$

$$\dot{m}_{CO_2} = k_{CO_2} \cdot \dot{m}_{fuel\,blend} \tag{3}$$

3 Driving cycle simplification methodology

The Worldwide harmonized Light vehicles Test Procedure (WLTP) is the current European standard to determine fuel consumption, and emissions of criteria pollutant and CO_2 light duty vehicles have (both combustion, hybrids and electric) [25]. It consists of chassis dynamometer tests cycles abbreviated as WLTC) that intend to reduce the discrepancies between the results obtained in the laboratory and real driving conditions. On this work, the Class 3 WLTC will be the focus as it is the cycle representative of light-duty vehicles driven in Europe. In particular, the Class 3b cycle will be evaluated, which has 4 phases, speeds above 120 km/h, a duration of 30 minutes and covers a distance of 23.25 km.

A methodology for the characterization of engine operation in the WLTC driving cycle is proposed based on a simplified cycle which only requires a limited amount of experimental data. In this approach the engine map is reduced to a few operating conditions following a discretization methodology that seeks to reproduce the results of the complete engine map with a limited and distributed dataset. The methodology allows for the reduction of experimental measurements while still providing insightful conclusions when correlated to a driving cycle, similarly to the work described in [20]. The interests in performing this kind of simplifications are the capability to work with limited resources, for example reduced fuel quantities or testing time, that could prevent the measurement of the complete engine map. For the case of this study the simplification of the engine map model needs to be able to apply a dedicated calibration strategy to each operating condition, which would be very cost and time intensive if the complete engine map was given the same treatment.

The methodology to reduce a complete engine map to a limited set of points must adhere to some considerations. Namely, the engine must already be characterized with at least one fuel. Namely, complete engine maps should be available. For the Diesel engine used in this study, because it is a commercial engine, information on the performance and fuel consumption was accessible to compare with the measurements and subsequently validate the proposed methodology. Additionally, measurements for the complete engine map were performed with diesel to have information on both the fuel consumption and main emissions that can later be compared with the results from the simplified methodology that uses only a few selected operating conditions.

3.1 Engine map characterization and GT-Power model

The complete engine map was characterized by measuring 35 stationary operating conditions distributed equally across the engine map with the diesel blend. The speed allocation was made every 500 rpm, starting at 1000 rpm and ending at 4000 rpm, while the load distribution was done every 10% of load at each speed. For each of these operating conditions fuel consumption and emissions where measured, as well as the instantaneous intake, exhaust and in-cylinder pressures and other boundary conditions. The experimentally obtained values where then used to feed a GT-Power vehicle model to calculate the WLTC (Figure 2).

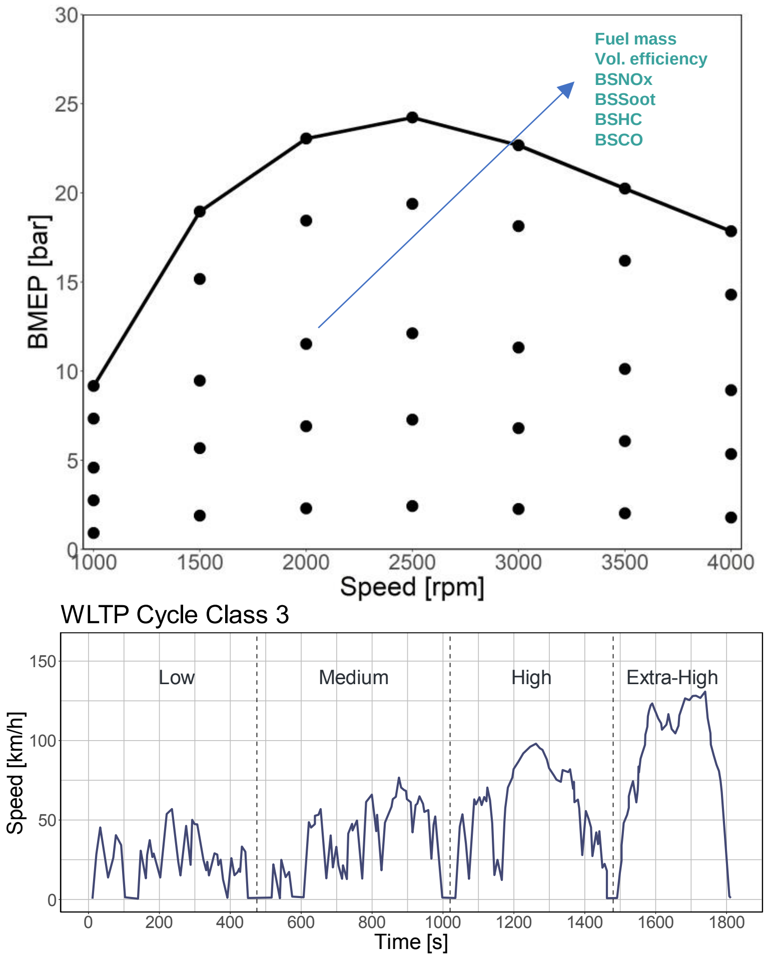

Figure 2 Input information for the GT-Power model. [Top] Experimentally measured engine map [Bottom] Speed profile for the Class 3b WLTC

For the GT-Power simulation, the vehicle modelled is an OPEL Astra J 1.6 CDT, which equips the engine that was described in the previous section.

Table 4 shows the aerodynamic and mechanical characteristics of the original equipment manufacturer (OEM) vehicle. Figure 3 illustrates the model and its sub-assemblies to represent the different vehicle systems. Each timestep speed profile is defined inside the object called “Driver”, which consists of a PID controller which acts on the accelerator position to provide the necessary power for the speed demand. Additionally, the object called “Engine-1” has the information on the engine fuel consumption and emissions that were experimentally measured, to be able to calculate these results across the cycle. The “Vehicle” template has all the information necessary to describe the operation, including the mass of both the vehicle and its cargo, the drag coefficient, the tire information including rolling resistance and differential information, as well as system strategies.

Table 4 Vehicle characteristics and driving strategy characteristics for the GT-Power modelling

Vehicle characteristics	
Base vehicle mass [kg]	1364
Passenger and cargo mass [kg]	145
Vehicle drag coefficient [-]	0.28
Frontal area [m^2]	2.8
Tires size [mm/%/inch]	225/50/R17
Differential ratio [-]	3.2
Wheelbase [cm]	268.5
Driving strategy	
Driver mode	Speed targeting
Transmission type	Manual
Gear shift-up [rpm]	2500
Gear shift-down [rpm]	1200

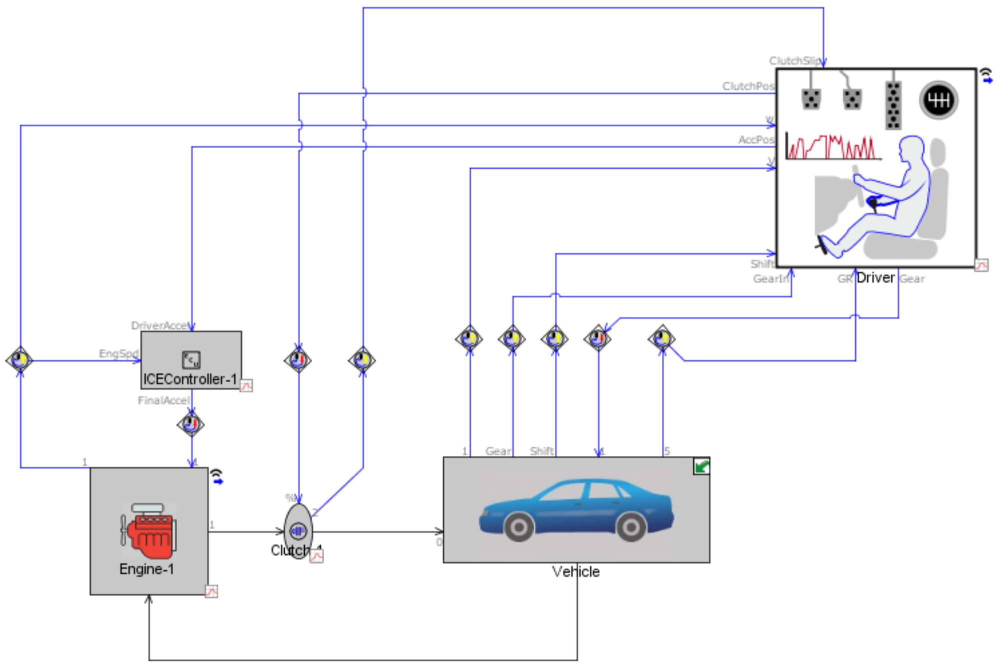

Figure 3 GT-Power vehicle model

For this study, the driver mode was set to speed targeting in order to be able to follow the speed profile of the WLTP cycle. With the model, the brake mean effective pressure (BMEP) and engine speed are determined for each instant, providing the information necessary to calculate the residence time for each engine operating condition (defined as the time the engine remains on a given speed and load). This output is represented in Figure 4, where it can be seen that most of the engine operation is concentrated at low loads and speeds, not exceeding 2500 rpm. It is important to highlight that the residence time results are dependent on the gear up shift strategy used, and the results may vary depending on whether a longer or shorter one is used.

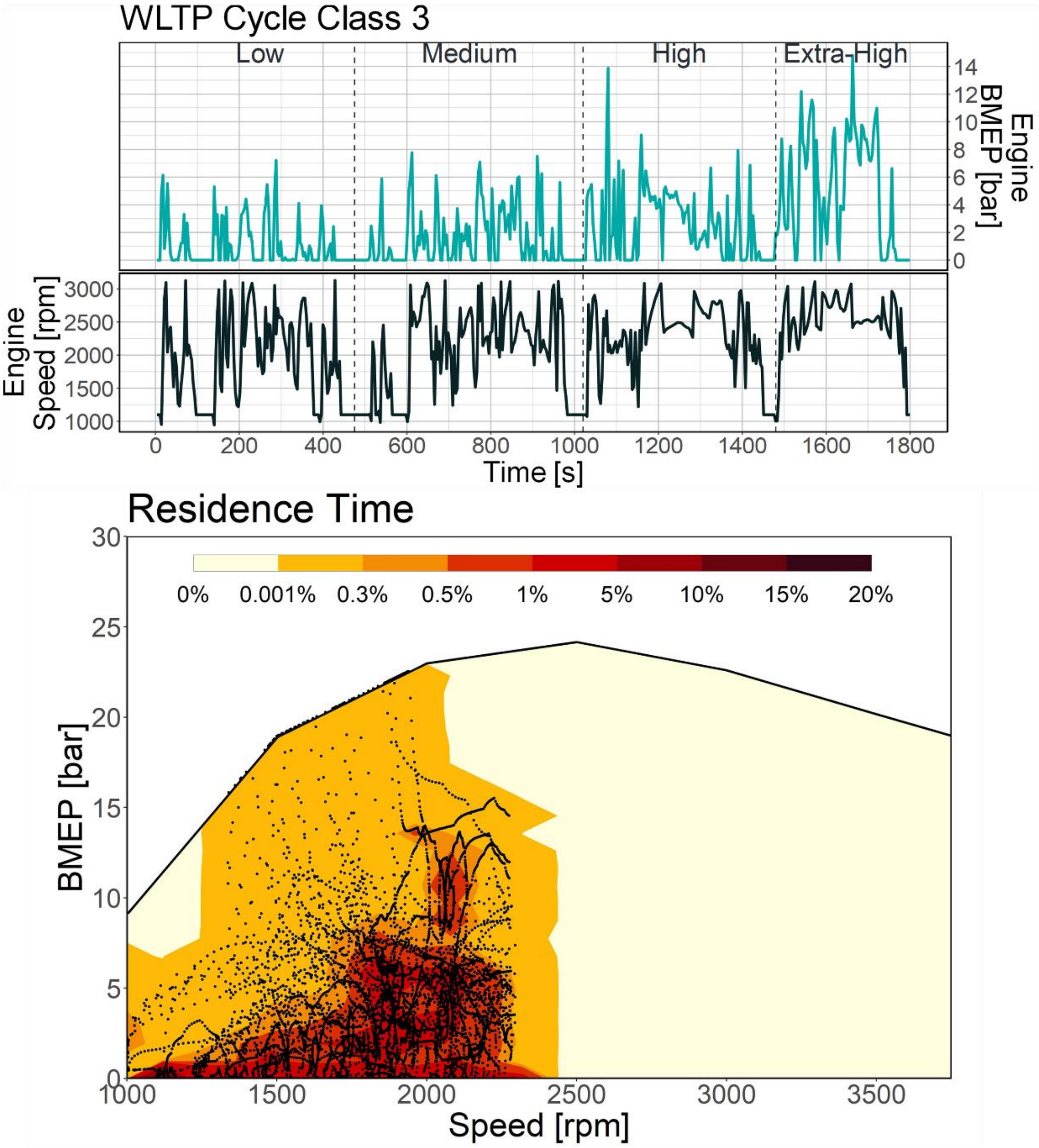

Figure 4 GT-Power model output [Top] Engine speed and load profiles [Bottom] Residence time map showing the distribution of operating conditions

3.2 Characterization of the engine map with limited operating conditions

Once the engine cycle operating conditions are characterized, it is desired to simplify the operation of the engine to a reduced quantity of operating points where each can be optimized individually, but a global overview of the driving conditions can still be obtained. The selected operating conditions for this study are based on the work of [26], and provide a low-speed low-load point, two mid-load points, and two high-load points. These operating conditions are distributed across the engine map in such a way that they can be representative of the engine operation. Table 5 describes the speed and BMEP for each one of the testing points.

Table 5 Engine operating conditions

Test Label	Speed [rpm]	BMEP [bar]	Cycle weight [%]
1250 rpm @ 2 bar	1250	2	52.00
1500 rpm @ 14 bar	1500	14	1.65
2000 rpm @ 8 bar	2000	8	44.42
2000 rpm @ 22 bar	2000	22	1.43

The simplification methodology for the WLTC cycle, is based on the discretization of the engine map into equal bin sizes with dimensions speed × load. The speed ranges cover a span of 500 rpm while the load is divided every 5 bar of BMEP (which is the maximum sized area that allows equally sized bins in the engine map), as can be seen in the first step in Figure 5. The second step of the process consists of using the operating conditions of interest as centroids, where multiple bins from the first step are grouped to form bigger bins that contain all the operating conditions of the cycle with their respective centroids. The bins in this step have a range of 1000 rpm and 10 bar of BMEP, and there can be overlap between them. To resolve the overlapping of bins and assign each of the centroids a unique area, the regions that overlap are divided in half, thus delimiting 4 singular regions within the engine map (as can be seen in the third step shown in Figure 5.

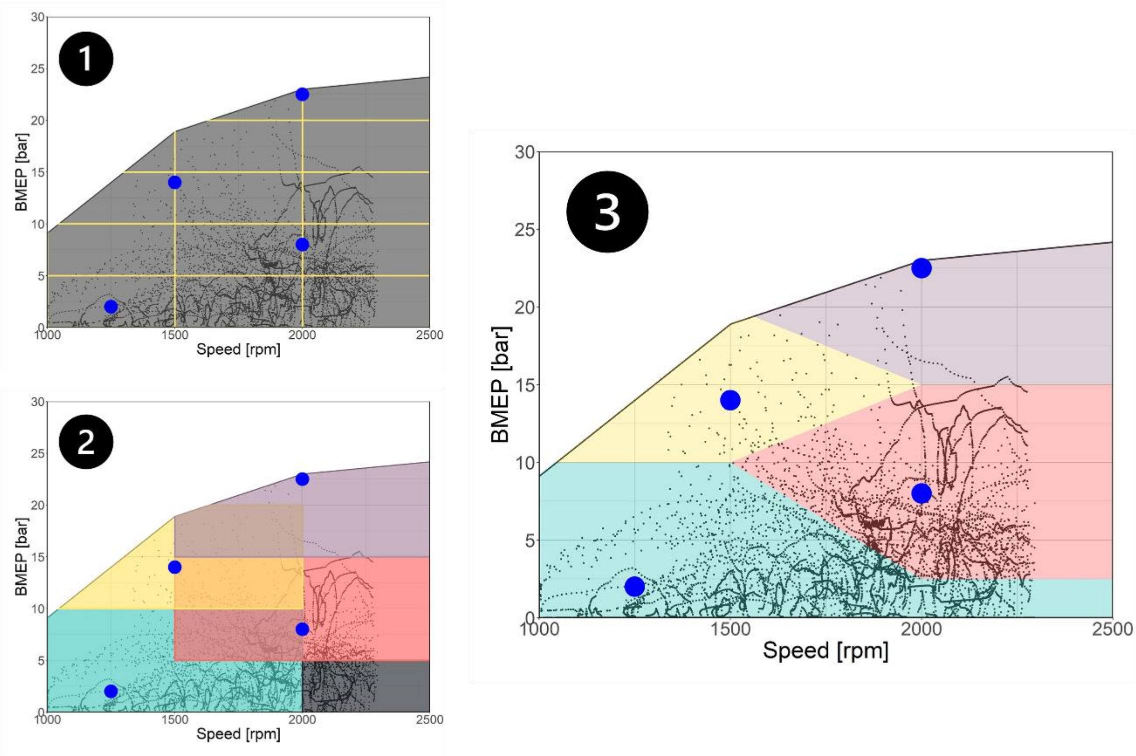

Figure 5 Engine map discretization procedure schematic

After the discretization in regions, the percentage of time within each region is calculated by counting the number of operating conditions that fall inside each area, where each point represents an equal amount of time in the respective condition. The proportion value is then assigned as the weight to be used in the simplified driving cycle that can be seen in Table 5. From both Table 5 and Figure 5, it should be noted how most of the weight of the cycle falls in the zones that correspond to the lower load operating conditions (1250 rpm @ 2 bar and 2000 rpm @ 8 bar).

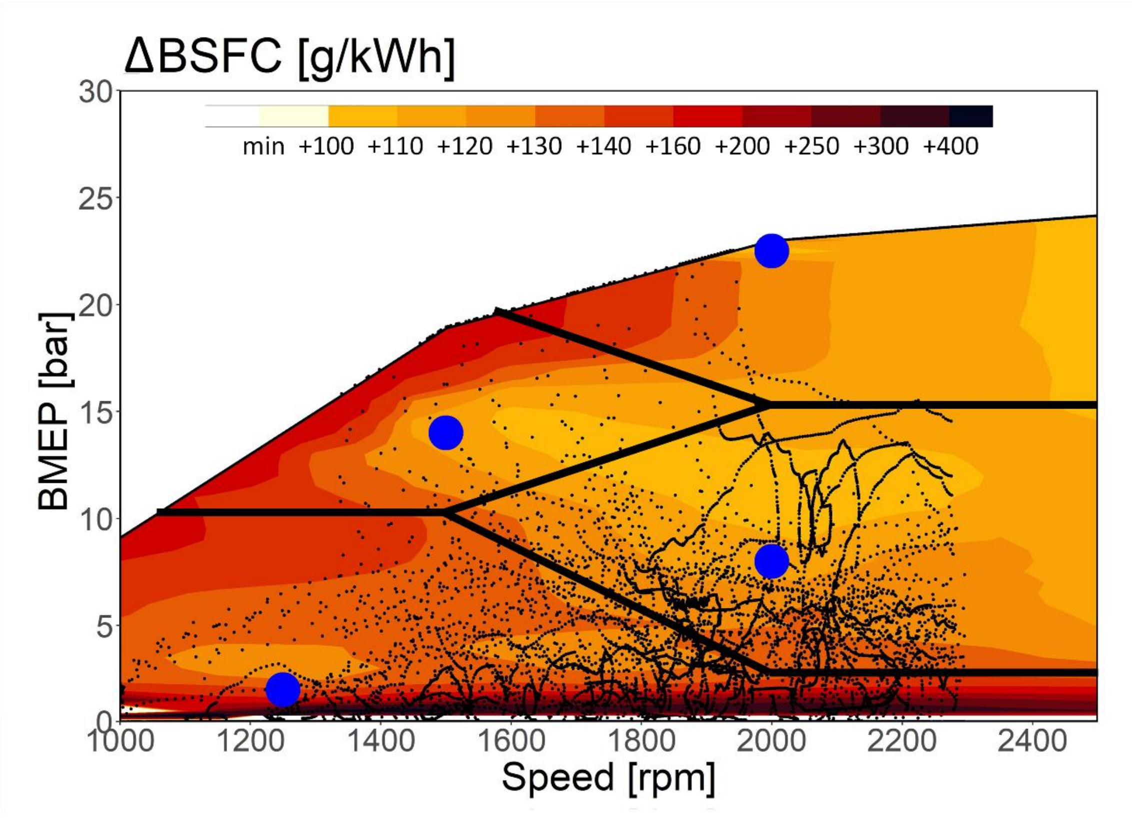

Figure 6 BSFC engine map and region delimitation after the discretization procedure. The blue dots represent the selected operating conditions for the discretized regions

Figure 6 shows the BSFC engine map which illustrates the different fuel consumption zones can be appreciated for the WLTC operating conditions. In the figure, it can be observed how the lower load conditions present the highest BSFC gradients and how, when the speed and load are increased, the variation in BSFC is less variable with lower values. This information is presented in Table 6, where the minimum, maximum and mean values of each region are given. It is also shown, how in terms of BSFC the selected operating conditions have values that are similar to the mean inside the corresponding region. To accept the proposed discretized regions, it was verified that the BSFC difference between extreme values and the selected operating point did not exceed 30% to ensure a good representation in terms of fuel consumption. In the same table, values for the main criteria pollutants can also be appreciated, highlighting that although the mean value for the region and the selected operating condition show relatively good agreement, emission values are harder to be represented with only a few stationary conditions. The results in Table 6 are presented as differences according to Equation 4 to preserve the intellectual property of the OEM.

$$\Delta X_{value} = X_{value} - X_{\substack{global \\ min}} \tag{4}$$

Table 6 Discretized engine map BSFC and emissions values represented as difference with respect to the global minimum value

		ΔBSFC [g/kWh]	ΔBSNOx [g/kWh]	ΔBSSoot [g/kWh]	ΔBSHC [g/kWh]	ΔBSCO [g/kWh]
Area 1 1250 rpm @ 2 bar	min	21.0	0.00	0.030	0.12	0.35
	max	502.9	3.02	4.886	6.01	13.22
	mean	80.8	1.55	0.455	0.82	4.21
	1250 rpm @ 2 bar	106.7	0.46	0.111	1.03	5.07
Area 2 1500 rpm @ 14 bar	min	2.2	0.19	0.051	0.02	0.97
	max	98.5	2.68	5.946	0.22	12.32
	mean	38.7	1.68	1.826	0.09	5.18
	1500 rpm @ 14 bar	36.1	1.43	0.066	0.07	3.83

Area 3 2000 rpm @ 8 bar	min	0.0	1.01	0.005	0.05	0.07
	max	34.5	4.63	0.104	0.66	4.40
	mean	17.0	2.16	0.053	0.16	0.91
	2000 rpm @ 8 bar	23.5	1.30	0.077	0.13	0.80
Area 4 2000 rpm @ 22 bar	min	5.8	0.19	0.000	0.00	0.00
	max	89.1	5.89	5.866	0.15	11.02
	mean	24.4	3.13	0.846	0.04	4.12
	2000 rpm @ 22 bar	26.8	2.71	0.348	0.02	10.07

3.3 Simplified engine map characterization validation results

With the selected operating conditions assigned their relative weight in the WLTC, the cycle calculation was performed and compared with the results yielded from the GT-Power model presented in previous sections. It has been shown in previous studies [27] that GT-Power models closely approximate experimentally measured driving cycle results for fuel consumption, but however struggle to accurately predict emissions due to the high effect transient operation has on pollutants, although relatively good approximation can be achieved for NOx emissions (difference below 4%) [28]. The results of the simplified cycle proposed in this study will be compared with the GT-Power results to serve as baseline of how well the methodology can provide information on a given driving cycle, with a small set of operating points. As an additional reference, the OEM-reported fuel consumption is also compared to have a fuller assessment of the results.

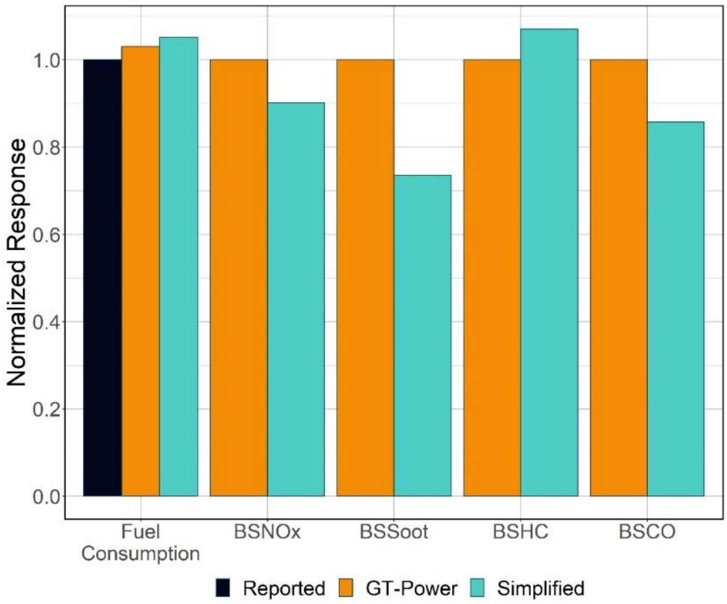

Figure 7 Simplified WLTP cycle results compared to the results obtained with the complete engine map GT-Power model and OEM reported fuel consumption values.

Figure 7 shows the simplified cycle results compared with the GT-Power model results and the OEM reported fuel consumption. In terms of fuel consumption, it can be noticed that the simplified methodology is around 5% higher than the reported values and 2% higher than the GT-Power results, which under real driving conditions is a feasible variation. Regarding the pollutant emissions it should be noted that the simplified cycle methodology shows lower values than GT-Power (except for HC), which under a real driving scenario are expected to be higher than GT-Power's results. Even though emissions might not be as well captured with this methodology as they would be with experimentally measured transient results, the simplified methodology provides a first insight into the emissions homologation potential of different fuels with a small operating point sample. The approach allows the characterization of the engine operation and the calculation of the CO_2 emissions of the engine in a given cycle, allowing the assessment of the carbon footprint of the engine. More importantly, having few operating conditions allows the calibration of each operating condition in a dedicated manner, as will be described in the following section.

4 Statistical model and optimization for a light-duty compression ignition engine

The current section will explain the engine optimization methodology. The methodology seeks to achieve a balance within the NOx-soot tradeoff prevalent in CI engines, while maintaining the highest possible efficiency and lowest fuel consumption using a low carbon fuel blend. The engine calibration process consists of defining various control parameters to obtain the desired responses from the engine in terms of emissions and performance. In this study the LCF blend, described in Table 3, will be evaluated and calibrated at the operation conditions corresponding to the simplified engine map areas (1250 rpm @ 2 bar, 1500 rpm @ 14 bar, 2000 rpm @ 8 bar and 2000 rpm @ 22 bar), without exceeding the constraints specified in Table 7 to guarantee a safe operation of the engine and, in the case of the emissions, to serve as targets for the optimization.

Table 7 Experimental constraints for the optimization of the testing operating conditions

Test Label	BSNOx [g/kWh]	Soot [FSN]	Pmax [bar]	PRR [bar/CAD]
1250 rpm @ 2 bar	0.2 — 1	< 2	<180	<8

1500 rpm @ 14 bar	<3	< 3	<180	<8
2000 rpm @ 8 bar	0.7 — 2	< 3	<180	<8
2000 rpm @ 22 bar	< 4.5	< 3	<180	<8

The study of each operating condition will be performed by a design of experiments (DoE) considering different variables corresponding to the fuel injection pressure, SOI of the main injection, the volume of the pilot injections, the dwell time between injections, as well as the air mass quantity and the boosting pressure. The design of experiments is done in two levels, a minimum and a maximum. The test matrix design depends on the operational condition; low and medium load conditions are explored with a 6-factor 2-k factorial design [29] with a central point, while the higher load points are studied with a modified Plackett-Burman design [30] with central points and also 6 factors. Both types of DoE allow to assess the interaction between factors. The use of two Plackett-Burmann design at higher loads follows the need for a shorter test run under these conditions. The shorter DOE promotes less permanence on straining engine conditions where in-cylinder and exhaust temperatures can be extremely high, or pressure rise rate (PRR) can surpass safety levels, and thus guarantees a safer engine operation, although the reduced amounts of test can slightly increase the error in the modeling. To overcome this issue, the modification on the Plackett-Burmann design is done by adding more experimental data points after the creation of a first model, where parameters necessary for the minimum achievable NOx, soot and BSFC operating conditions are found, as well as maximum efficiency and an efficiency-emissions-fuel consumption balanced operating point are found. The prediction accuracy is later checked in the engine. If after the initial screening, the operating conditions responses have an accuracy of less than 90%, this process is repeated, adding the new experimental results into the data set and finding new parameters until the error is below 10%.

As can be seen in Figure 8, the different operating conditions use different injection strategies which can include one or two pilot injections. The cases with two pilot injections, which are the lower load points, have 8 possible variable parameters, however for the study only 6 were modified during the optimization and the other 2 remained fixed. Additionally, it was important to know beforehand the minimum and maximum levels achievable with each parameter. For those reasons, preliminary tests were performed with two defined objectives: individually test each factor to see the limit at which the previously mentioned constraints are exceeded (which consequentially allows to ensure a monotonous behavior); and provide a factor removal criterion, based on the standardized response of each parameter, for the operating conditions that have two pilot injections.

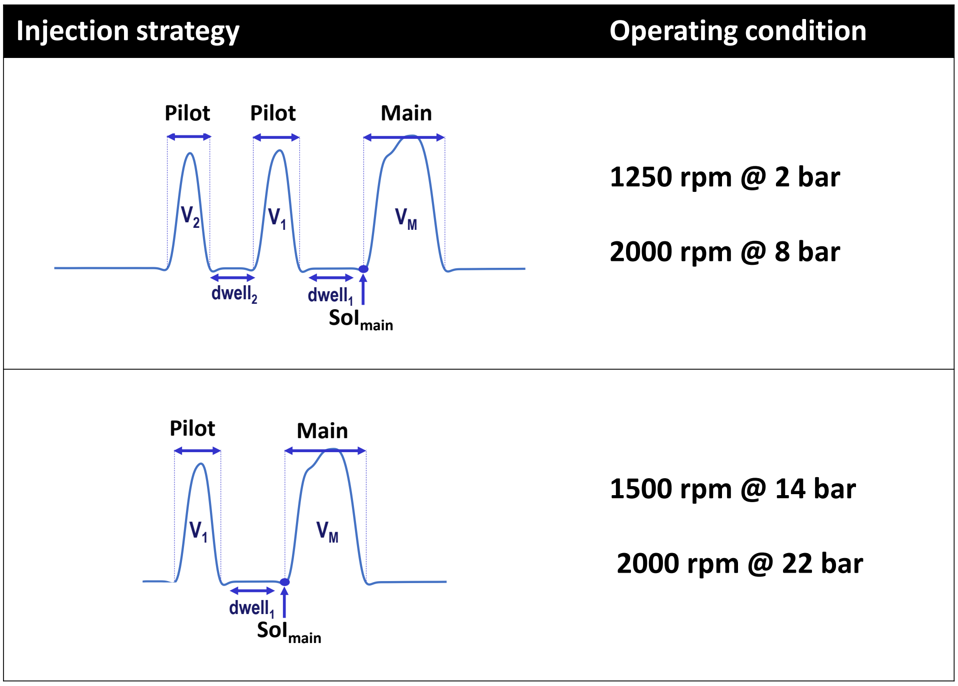

Figure 8 Injection strategy for the different tested operating conditions

The factor removal criteria involve the evaluation of the standardized effect [31] of the variables on the responses of BSNOx, gross brake efficiency (GBE), BSFC and soot (in FSN number). To select which variables to remove the responses are normalized and combined according to equation 5. On the equation, SR_x is the standardized effect of a parameter x on a given response [32] [33]; which is normalized to equally weight the effects of interest, and CR the combined sized effect for each of the parameters studied.

$$CR = \sum_{y=responses} \frac{|SR_x|}{\max(|SR_x|)_{response}} \qquad (5)$$

The combined sized effect results for both low load points can be seen in Figure 9, where for the single parameter tests on the operating condition 1250 rpm @ 2 bar the boosting pressure (represented as VGT) and the rail pressure have the least significant effect and will thus be kept fixed. While, for the operating point 2000 rpm @ 8 bar it is observed how the variation of the characteristics of the second pilot injection have the least important effect.

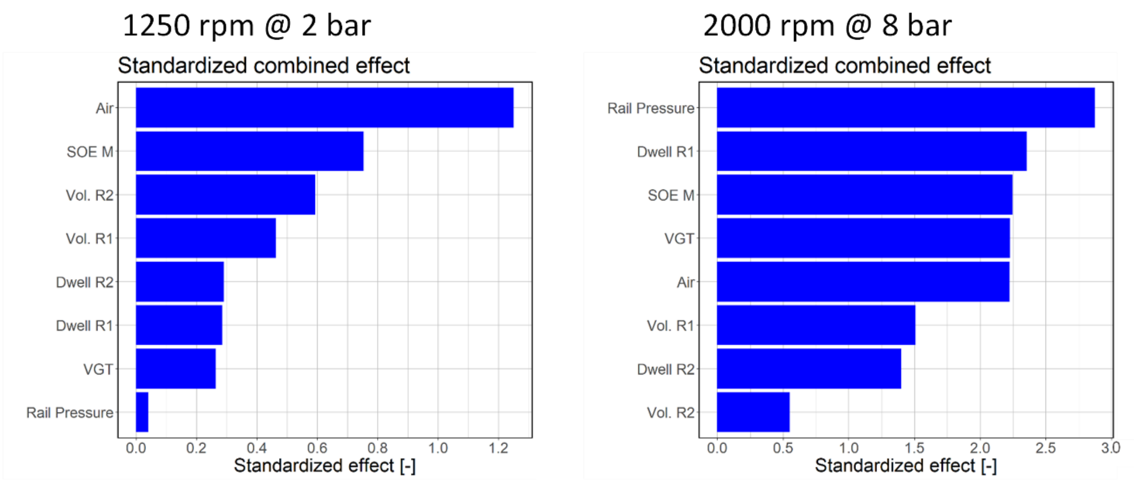

Figure 9 Standardized responses for the operating conditions with two pilot injections to define which 6 factors are studied during the calibration procedure with an LCF blend

After selecting the variables to test for each of the operating conditions, the variables and their testing levels can be seen in Table 6. And, in accordance with the types of DoE selected, different combinations of the factor levels are observed to better understand the parameter effects.

Table 8 Experiment design matrix with variables and levels

Variable	1250 rpm @ 2 bar	1500 rpm @ 14 bar	2000 rpm @ 8 bar	2000 rpm @ 22 bar
SoI [deg bTDC]	[-4; 5.5; 7]	[-4; 0; 4]	[2; 5; 8]	[5; 8; 11]
Rail Pressure [bar]	[240; 275; 310]	[800; 875; 950]	[780; 860; 940]	[1050; 1150; 1250]

Vol. pilot 1 [mm^3]	[0.9; 1.4; 1.9]	[1.0; 2.0; 3.0]	[0.9; 1.6; 2.3]	[1.2; 1.8; 2.4]
Dwell pilot 1 [ms]	[0.680; 0.723; 0.765]	[0.500; 0.75; 1.000]	[0.590; 0.700; 0.810]	[1.000; 1.250; 1.500]
Vol. pilot 2 [mm^3]	[0.9; 2.0; 3.0]	[-]	[0.9; 1.7; 2.4]	[-]
Dwell pilot 2 [ms]	[0.630; 0.710; 0.790]	[-]	[0.500; 0.600; 0.700]	[-]
Air [mg]	[180; 196; 212]	[610; 625; 640]	[412; 424; 435]	[610; 625; 640]
Boost pressure [kPa]	[102; 103.5; 105]	[162; 171; 180]	[140; 150; 160]	[162; 171; 180]
Type of DOE	2-k factorial with center	Modified Plackett-Burman	2-k factorial with center	Modified Plackett-Burman

4.1 Statistical analysis and model development

The design of experiments allows to obtain polynomial regression equations that follow the form shown in Equation 6. The regressions represent the responses obtained by the variation of the different factors. The b_0 coefficient is the mean of the analyzed responses, while coefficients b_i and b_{ij} represent the effect of the variables X_i and the interaction between X_iX_j, respectively. Interaction between factors was limited to only first order interactions (b_{ij}), or coefficient of effectiveness of second grade, due to this being able to represent the main effects without providing excessive degrees of freedom to the model.

$$Y = b_0 + \sum_{i}^{k} b_i X_i + \sum_{i}^{k} \sum_{j \neq i}^{k} b_{ij} X_i X_j \qquad (6)$$

The best polynomial model was selected for each of the responses of interest and each operating condition, including the mechanical constraint responses. The final polynomial equation for each case was then used to obtain the curve predicted by the model. The polynomial models obtained contain only significant terms (following the convention of $p < 0.05$), r-square above 80% and an F-statistic that allows the rejection of the null hypothesis.

4.1.1 Model evaluation

One of the main interests in generating model is to be able to characterize the engine behavior with the modification of the different parameters and to be able to predict the conditions necessary to obtain a combustion that fulfills the constraints criteria, while also maintaining good performance and efficiency values. That objective demands that the models can closely reflect experimental values. Table 9 shows the r-square values for the main responses indicating there is good agreement between both experimental and modelled values. It is important to highlight that the accuracy of the models can only be ensured within the ranges studied.

Table 9 R-square values for the main studied responses across all operating conditions

	BSNOx	Soot	BSFC	GBE
1250 rpm @ 2 bar	93.8	84.1	82.2	83.9

1500 rpm @ 14 bar	95.6	85.9	89.4	91.2
2000 rpm @ 8 bar	99.4	93.0	91.2	96.8
2000 rpm @ 22 bar	95.1	92.1	90.4	83.3

4.2 Operating condition optimization based on modelling results

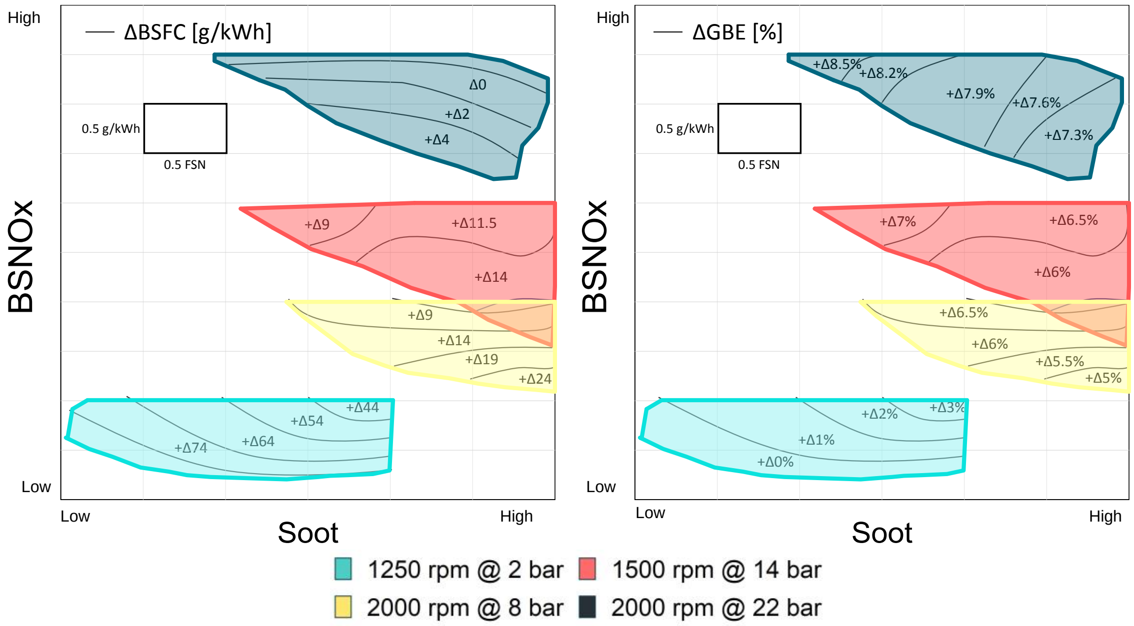

Figure 10 BSNOx-FSN tradeoff [Left] Including BSFC maps; [Right] Including GBE maps. Values are expressed as absolute differences following the convention specified in equation 4.

The developed models for the different responses allow the augmentation of the data to test not experimentally measured operating conditions. Figure 10 shows the relation between the modelled NOx and soot emissions for the operating conditions that comply with the previously defined constraints. In terms of emissions, it can be seen how the

NOx emissions increase when the load is increased. The 1250 rpm @ 2 bar condition has both the lowest NOx and soot emissions . The relation between BSFC and the emissions' tradeoff is also reflected in the figure. It can be observed that within each operating condition the increased in NOx is inversed to the fuel consumption increase; when the BSFC is reduced, the BSNOx are increased and vice versa. The correlation with soot, however, is not as strong. Similar inferences can be extracted from the GBE maps; the difference being that for the operating condition 2000 rpm @ 22 bar a well-defined correlation is found between GBE and soot, where a reduction of 1 FSN can see an increase of 0.6% of efficiency.

This work also intends to propose an optimized operating condition that has both low NOx and soot emissions. As these two emissions present a strong tradeoff between them, the implementation of optimization criteria is necessary to select the best operating condition. Additionally, it is of interest to be able to have the highest possible GBE and the lowest BSFC. The operating condition is selected by applying the optimization functions described on equations 7 to 10. In these equations, ϵ is the admissible threshold for the desired response. To achieve an optimum and balanced point (an operating condition with lowest possible NOx, soot, fuel consumption and the highest efficiency), the minimum ϵ is found so that only one value fulfills all conditions.

$$BSNOx < BSNOx_{min}(1 + \epsilon) \quad (7)$$

$$BSSoot < BSSoot_{min}(1 + \epsilon) \quad (8)$$

$$BSFC < BSFC_{min}(1 + \epsilon) \quad (9)$$

$$GBE > GBE_{max}(1 - \epsilon) \quad (10)$$

The optimized point for each of the operating conditions can be seen in Table 10. The values from the model were later experimentally measured to verify the accuracy and precision of said model. From the optimized values, it can be mentioned that the SoI is delayed (within the specified limits) for all operating conditions, which is an injection strategy that helps in the reduction of NOx emissions. Regarding the other variables, no specific trend can be detected in terms of injection pressure, pilot injection characteristics nor air management characteristics. The table also includes the responses with their respective confidence interval for the model and the measurement error for the experimental values. From the table, good agreement between predicted and measured values can be seen. Responses are again presented as differences following Equation 4.

Table 10 Optimized operating conditions settings and normalized results for both modelled and experimental responses with their associated errors.

Settings				
Variable	1250 rpm @ 2 bar	1500 rpm @ 14 bar	2000 rpm @ 8 bar	2000 rpm @ 22 bar

SoI [deg bTDC]		-4	2	2	5.5
Rail Pressure [bar]		290	860	940	1050
Vol. pilot 1 [mm^3]		1.9	1.0	1.8	1.2
Dwell pilot 1 [ms]		750	500	630	1000
Vol. pilot 2 [mm^3]		0.85	-	1.3	-
Dwell pilot 2 [ms]		790	-	600	-
Air [mg]		180	640	435	850
Boost pressure [kPa]		103.7	180	156	245
Responses					
ΔBSNOx [g/kWh]	Mod.	0.1±0.1	2.1±0.1	1.24±0.08	3.6±0.1
	Exp.	0.0±0.2	2.2±0.1	1.11±0.08	3.7±0.1
ΔBSSoot [g/kWh]	Mod.	0.00±0.01	0.02±0.01	0.15±0.01	0.06±0.01
	Exp.	0.03±0.05	0.03±0.07	0.21±0.06	0.09±0.03
ΔBSFC [g/kWh]	Mod.	65±2	13±4	14.0±2	0±2
	Exp.	70±7	11±2	12±2	5±2
ΔGBE [%]	Mod.	0.9±0.3	7.0±0.7	7.1±0.2	8.9±0.2
	Exp.	0.0±0.7	7.5±0.3	7.2±0.3	8.4±0.3

5 Application of simplified WLTC cycle for the evaluation of an LCF blend

After the optimization of the operating conditions in section 4, the simplified driving cycle shown in section 3 is applied to first estimate the potential of the LCF to be able to fulfill Euro 6 emissions and to calculate the potential CO_2 reductions that can be achieved by the use of a fuel with 33% volumetric renewable content. Figure 11 shows the main pollutants divided by their Euro 6 limits. In the figure it should be highlighted that Euro 6 limits are not fulfilled. For the case of NOx, the cycle emissions with the LCF are around 1.75 times the Euro 6 limit. On the other side, soot emissions are over 6 times the admissible limit. Regarding the products of incomplete combustion (HC and CO) the Euro 6 limit is exceeded by 1.5 and 2.8 times respectively. Although emissions are not fulfilled, is important to remember that the values here presented correspond to engine-out values, thus some improvement regarding emissions can be achieved if an aftertreatment system were to be considered. In the case of soot particulates, it has been reported that diesel particulate filters (DPF) can have efficiencies beyond 95% [34]. A DOC in turn would oxidize big part of CO and HC reported efficiencies of 90% [24]. Assessing these aftertreatment scenarios it is feasible to consider that emissions can be fit into Euro 6, although further dedicated testing is desired to confirm this hypothesis. Additionally, it is worth considering that high soot levels would require some maintenance for the DOC at more frequent intervals than with the current baseline calibration.

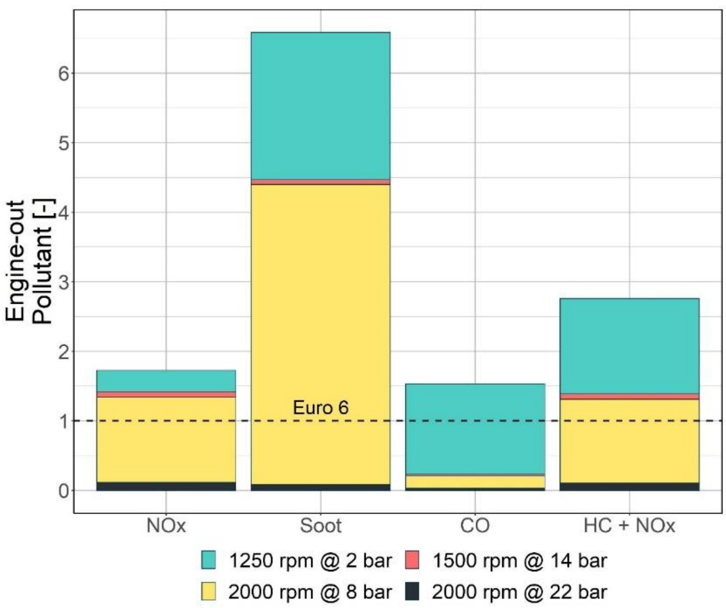

Figure 11 Cycle engine-out criteria pollutants normalized by the Euro 6 regulation limits

In Figure 12 the fuel consumption can be seen with a value of 1 as the results are normalized for that response. However, when applying Equation 1, the fuel consumption of the LCF can be evaluated with a correlation to commercial diesel, finding that the studied LCF has only 0.54% higher fuel consumption than diesel if both contained the same amount of energy by mass. Another important result that can be obtained with the simplified WLTC are the fuel consumption and CO_2 emissions including Well-to-Tank (WTT), Tank-to-Wheel (TTW) and Well-to-Wheel (WTW). The studied fuel is carbon negative due to its 33% volumetric renewable content, and thus the equivalent WTT CO_2 has a negative value. This implies that the fuel production removes more CO_2 from the atmosphere than it emits. On the other hand, the TTW emissions are 3.13 the fuel mass which is directly extracted from the coefficient shown in Table 3. Finally, in terms of WTW a slight reduction can be appreciated compared to TTW due to the added effect of the negative WTT value, however this reduction corresponds only to 4.8% reduction in the total equivalent CO_2.

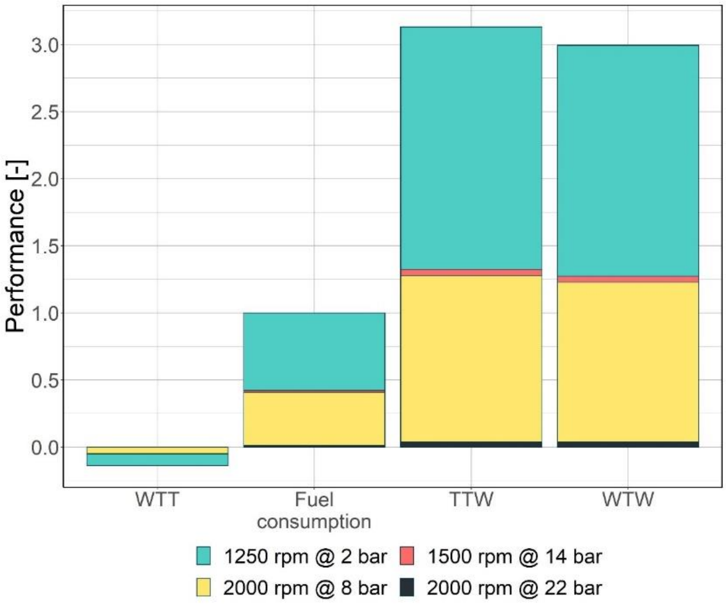

Figure 12 Fuel consumption and CO_2 equivalent emissions normalized by the fuel consumption of the engine

6 Summary and conclusions

This study compiled the description of a simplified driving cycle methodology to evaluate the performance of a given engine using only a few experimental conditions and the calibration of such operating conditions using polynomial models and statistical analysis. From the combination of both methodologies the optimization and assessment of an LCF blend was possible within a commercially available Diesel engine. The main attractive for the use of a simplified methodology to evaluate a driving cycle is the avoidance of the calibration of the complete engine map (in favor of the calibration of only a few selected conditions), which can be a costly and time extensive procedure; in particular, when evaluating LCFs whose operation and characteristics have to be explored in a more intensive manner and for which large quantities are difficult to procure due to their experimental nature.

Regarding the optimization process, it was confirmed that the engine operation can be refined to fulfill specific constraints with a DoE with variation of defined parameters, and subsequent statistical modelling. In particular, is possible to comply with the limitation of NOx and soot emissions, which are two of the main pollutants in CI engines. Finally, an optimization function is presented that sought to find the most balanced operating condition in terms of NOx, soot, BSFC and GBE.

From the results obtained in this study, it can be highlighted that:

- The simplified WLTC methodology shows good agreement with OEM reported fuel consumption and GT-Power model driving cycle simulations (around 5% of deviation).
- The created models and experimental values are very close in terms of BSFC, BSNOx, BSSoot, BSHC and BSCO. Additionally, is observed how the confidence interval of the models overlaps with experimental values when considering experimental error
- Although engine-out Euro 6 main criteria pollutant emissions are not compliant, the application of an aftertreatment system will let the emissions fulfill Euro 6.
- Using an LCF with 33% renewable content, and properties similar to diesel fuel, a reduction of 4.8% equivalent WTW CO_2 can be obtained, when compared with TTW emissions due to the use of atmospheric CO_2 during the fuel production process, which is reflected with a negative WTT CO_2 value.

Acknowledgments

The authors thank ARAMCO Overseas Company for supporting this research.

References

[1] H. Ritchie, "Emissions by sector," 2018. [Online]. Available: https://ourworldindata.org/ghg-emissions-by-sector. [Accessed 28 June 2021].

[2] IRENA, "Renewable capacity statistics 2021," International Renewable Energy Agency (IRENA), Abu Dhabi, 2021.

[3] IEA, "Projected Costs of Generating Electricity 2020," IEA, Paris, 2020.

[4] M. Segreto, L. Principe, A. Desormeaux, M. Torre, L. Tomassetti, P. Tratzi, V. Paolini and F. Petracchini, "Trends in Social Acceptance of Renewable Energy Across Europe—A Literature Review," *International Journal of Environmental Research and Public Health,* vol. 17, no. 24, p. 9161, 2020.

[5] IEA, "Global EV Outlook 2021," IEA, Paris, 2021.

[6] M. Taylor, "EU Suggests Date For The End Of Combustion-Powered Cars, SUVs," *Forbes,* 14 July 2021.

[7] A. Arora, N. Niese, E. Dreyer, A. Waas and A. Xie, "BCG," 20 April 2021. [Online]. Available: https://www.bcg.com/publications/2021/why-evs-need-to-accelerate-their-market-penetration.

[8] M. Williams and R. Minjares, "A technical summary of Euro 6/VIvehicle emission standards," icct - The International Council on Clean Transportation, 2016.

[9] R. M. Cuéllar-Franca and A. Azapagic, "Carbon capture, storage and utilisation technologies: A critical analysis and comparison of their life cycle environmental impacts," *Journal of CO_2 Utilization,* vol. 9, pp. 82-102, 2015.

[10] M. Marchese, G. Buffo, Santarelli and A. Lanzini, "CO_2 from direct air capture as carbon feedstock for Fischer-Tropsch chemicals and fuels: Energy and economic analysis," *Journal of CO_2 Utilization,* vol. 46, p. 101487, 2021.

[11] C. Luna, D. Luna, J. Calero, F. Bautista, A. Romero, A. Posadillo and V.-E. C., "7 - Biochemical catalytic production of biodiesel," in *Handbook of Biofuels Production (Second Edition)*, Woodhead Publishing, 2016, pp. 165-199.

[12] H. Aatola, M. Larmi, T. Sarjovaara and S. Mikkonen, "Hydrotreated Vegetable Oil (HVO) as a Renewable Diesel Fuel: Trade-off between NOx, Particulate Emission, and Fuel Consumption of a Heavy Duty Engine," *SAE Int. J. Engines,* vol. 1, no. 1, pp. 1251-1262, 2009.

[13] J. Preuß, K. Munch and I. Denbratt, "Performance and emissions of renewable blends with OME3-5 and HVO in heavy duty and light duty compression ignition engines," *Fuel,* vol. 303, p. 121275, 2021.

[14] G. Rao, G. N. Kumar and M. Herbert, "Effect of injection pressure on the performance and emission characteristics of the CI engine using Vateria indica biodiesel," *International Journal of Ambient Energy,* vol. 40, no. 7, pp. 758-767, 2017.

[15] K. Dev Choudhary, A. Nayyar and M. Dasgupta, "Effect of compression ratio on combustion and emission characteristics of C.I. Engine operated with acetylene in conjunction with diesel fuel," *Fuel,* vol. 214, pp. 489-496, 2018.

[16] J. Hwang, D. Qi, Y. Jung and C. Bae, "Effect of injection parameters on the combustion and emission characteristics in a common-rail direct injection diesel engine fueled with waste cooking oil biodiesel," *Renewable Energy,* vol. 63, pp. 9-17, 2014.

[17] M. Valihesari, Pirouzfar, F. Ommi and F. Zamankhan, "Investigating the effect of Fe2O3 and TiO2 nanoptaticle and engine variables on the gasoline engine performance through statistical analysis," *Fuel,* vol. 254, p. 115613, 2019.

[18] E. H. Brahmi, L. Denis-Vidal, Z. Cherfi and N. Boudoud, "Statistical modeling and optimization for diesel engine calibration," *35th Annual Conference of IEEE Industrial Electronics,* pp. 1770-1775, 2009.

[19] A. García, J. Monsalve-Serrano, S. Martínez-Boggio, P. Gaillard, O. Poussin and A. A. Amer, "Dual fuel combustion and hybrid electric powertrains as potential solution to achieve 2025 emissions targets in medium duty trucks sector," *Energy Conversion and Management,* vol. 224, p. 113320, 2020.

[20] A. García, J. Monsalve-Serrano, D. Villalta and M. Guzmán Mendoza, "OMEx Fuel and RCCI Combustion to Reach Engine-Out Beyond the Current EURO VI Legislation," *SAE Technical Paper,* 2021.

[21] ETAS Driving Embedded Excellence, "INCA Software Products," ETAS Driving Embedded Excellence, [Online]. Available: https://www.etas.com/en/products/inca_software_products.php. [Accessed 30 September 2021].

[22] M. Yugo, V. Gordillo, E. Shafiei and A. Megaritis, "A look into the life cycle assessment of passenger cars running on advanced fuels," in *SIA Powertrain & Electronics conference*, France, 2021.

[23] J. Benajes, A. García, J. Monsalve-Serrano and R. Sari, "Evaluating the Efficiency of a Conventional Diesel Oxidation Catalyst for Dual-Fuel RCCI Diesel Gasoline Combustion," *SAE Technical Paper,* vol. 01, no. Sept, p. 1729, 2018.

[24] A. Ayodhya and K. Narayanappa, "An overview of after-treatment systems for diesel engines," *Environ Sci Pollut Res Int,* vol. 25, no. 35, pp. 35034-35047, 2018.

[25] P. Mock, "World-Harmonized Light-Duty Vehicles Test Procedure," 22 11 2013. [Online]. Available: https://theicct.org/publications/world-harmonized-light-duty-vehicles-test-procedure.

[26] R. Durrett and M. Potter, "Renewable Energy to Power through Net-Zero-Carbon Fuels," in *THIESEL 2020 Conference on Thermo- and Fluid Dynamic Processes in Direct Injection Engines 8th-11th September 2020*, Valencia, 2020.

[27] A. García, J. Monsalve-Serrano, S. Martínez-Boggio, P. Gaillard, O. Poussin and A. A. Amer, "Dual fuel combustion and hybrid electric powertrains as potential solution to achieve 2025 emissions targets in medium duty trucks sector," *Energy Conversion and Management,* vol. 224, p. 113320, 2020.

[28] J. M. Luján, A. García, J. Monsalve-Serrano and S. Martínez-Boggio, "Effectiveness of hybrid powertrains to reduce the fuel consumption and NOx emissions of a Euro 6d-temp diesel engine under real-life driving conditions," *Energy Conversion and Management,* vol. 199, p. 111987, 2019.

[29] D. C. Montgomery, Design and Analysis of Experiments, 10th Edition, New York: John Wiley, 2019.

[30] Analytical Methods Committee AMCTB No 55, "Experimental design and optimisation (4): Plackett–Burman designs," *Anal. Methods,* vol. 5, no. 8, pp. 1901-1903, 2013.

[31] Transparent Statistics in Human–Computer Interaction working group, Transparent Statistics Guidelines, 2019.

[32] J. Lawson, Design and Analysis of Experiments with R, New York: Chapman and Hall/CRC, 2015.

[33] A. Field, J. Miles and Z. Field, Discovering Statistics Using R, London: SAGE Publications, 2012.

[34] B. Guan, R. Zhan, H. Lin and Z. Huang, "Review of the state-of-the-art of exhaust particulate filter technology in internal combustion engines," *Journal of Environmental Management,* vol. 154, pp. 225-258, 2015.

[35] O. A. Kuti, S. M. Sarathy and K. Nishida, "Spray combustion simulation study of waste cooking oil biodiesel and diesel under direct injection diesel engine conditions," *Fuel,* vol. 267, p. 117240, 2020.

Abbreviations

BMEP	Brake mean effective pressure
CI	Compression ignition
DOC	Diesel oxidation catalyst

DOE	Design of experiments
DPF	Diesel particulate filter
EV	Electric vehicle
FAME	Fatty acid methyl esters
GBE	Gross brake efficiency
HC	hydrocarbons
HVO	Hydrogenated vegetable oil
ICE	Internal combustion engine
LCF	Low carbon fuel
LHV	Lower heating value
OEM	Original equipment manufacturer
PM	Particulate matter
PRR	Pressure rise rate
SI	Spark ignition
SOI	Start of injection
TTW	Tank-to-wheel
WLTC	World harmonized Light vehicle Test Cycle
WLTP	World harmonized Light vehicle Test Procedure
WTT	Well-to-tank
WTW	Well-to-wheel